Precise life-time prediction using demarcation energy approximation for distributed activation energy reaction

2006 J. Phys.: Condens. Matter 18 2199

(http://iopscience.iop.org/0953-8984/18/7/009)

INSTITUTE OF PHYSICS PUBLISHING JOURNAL OF PHYSICS: CONDENSED MATTER

J. Phys.: Condens. Matter **18** (2006) 2199–2216 doi:10.1088/0953-8984/18/7/009

Precise life-time prediction using demarcation energy approximation for distributed activation energy reaction

B Poumellec[1], I Riant[2] and C Tessier-Lescourret[2]

[1] LPCES UMR CNRS-UPS 8648, Université de Paris Sud, 91405 Orsay Cedex, France
[2] Alcatel CIT, 7-9 Avenue Morane Saulnier, BP 57 78141 Vélizy, France

Received 25 July 2005, in final form 11 January 2006
Published 2 February 2006
Online at stacks.iop.org/JPhysCM/18/2199

Abstract

The requirement from the industry of precise lifetime estimation of Bragg gratings in optical fibres and other optical devices motivated us to perform calculations in a region of a master curve (describing the time evolution of a system at any temperature) where an approximation, called demarcation energy, is no longer valid. We describe a correction procedure that leads to reintroducing afterwards a temperature dependence lost in this approximation while preserving most of the advantages of the demarcation energy approach. With our procedure, a precise determination of burning-in parameter for achieving lifetime specification is possible.

A Bragg grating written in H_2 loaded Ge doped silica core optical fibres is used as application example.

(Some figures in this article are in colour only in the electronic version)

1. Introduction

The development of Bragg gratings inscripted in optical fibres by means of a UV laser is an important breakthrough in optical fibre communication in the last few years. After various trials for enhancing the photosensitivity in optical fibres, the industrials have converged at the moment on the writing in optical fibres with a H_2 loaded Ge doped silica core, awaiting further improvement from basic research. Meanwhile, it seems necessary to improve the estimate of the lifetime from a wealth of experimental data which is available with ever increasing precision.

For modelling the relaxation process in disordered media, several approaches can be used; an extended report can be found in the reference book of Richert and Blumen [1]. The main problem that one encounters in each of these approaches is to account for the effect of disorder on the relaxation processes. Indeed, the disorder can affect the various steps of a physico-chemical reaction, allowing the relaxation of the observed quantity. For instance, if

hopping is considered in a reaction, the disorder will appear on the hopping distance or on the waiting time. On the other hand, if an energy barrier is involved, the activation energy will be distributed because the transition and/or the stable state configurations are numerous. These two examples differ fundamentally on one point: the temperature will affect the range limited or the temperature activated hopping differently. In particular, the dependence of the stability of the refractive index with the writing or the ageing temperature [2] can only be explained by processes with distributed activation energies. Other arguments connected to structural changes also reinforce this conclusion. However, a process like decoration of network defects with hydrogen atoms will not necessarily be relevant to a thermally activated process and exponents appearing in non-exponential laws like the stretched exponential will be related in this case to the fractal nature of the defect structure space. In this paper, we consider only those relaxation processes involving distribution of activation energies. As it is seen, this approach yields good results [3, 4] in problems of index change.

The method now widely used in the field of optical fibres introduced by Lemaire *et al* in 1984 [5] for hydrogen induced darkening and by Erdogan *et al* in 1994 [3, 6] for Bragg grating stability has its foundation in numerous previous works which began with the study of the electric discharge in a Leyde jar due to Kohlrausch in 1847 [7]. He found a stretched exponential behaviour with an exponent of 0.43. Later in 1876, Hopkinson [8] proposed another relaxation function for a dielectric: Bt^{-n}. In 1893, Wiechert [9] suggested that relaxation energies in solids are distributed according to a Gaussian curve. In 1907, Von Schweidler [10] introduced the concept of relaxation time. In 1913, Wagner [11] suggested that the relaxation time was governed by a probability function which he assumed to have a Gaussian line shape distribution. At this juncture, Vand [12] proposed two experimental methods for studying the activation energy distribution (of what he called 'lattice distortions', actually): the isothermal and tempering annealing. He defined a cutting energy for an energy distributed first order kinetics and showed that the distribution function is the derivative of the produced quantity according to this energy; he also studied the error introduced by this approximation. This was an important step forward in the study of disordered media but the role of the demarcation energy remained eluded and so also a correction method. In 1955, Primak [13] extended the Vand approach by defining a 'characteristic activation energy' (in fact, what will be called the demarcation energy later) and extended the field of application to investigate kinetics with order larger than one, but he noted that the first order kinetics is the most likely scenario in solids. In 1960, Primak [14] continues studying the isochronous method which was an improvement over the Vand method. He made many investigations in silica, especially about radiation induced compaction or dilatation. Since then, several publications dealing with distributed kinetics have appeared in the literature but without any mention of the original works. Tiedje *et al* (1980) and Orenstein *et al* (1981) [15, 16] invoked a demarcation energy which is actually the Vand cutting energy. In 1991, Miller [17] developed a predictive formalism to describe generalized activated physical processes. In 1992, Lemaire [18], and in 1994, Erdogan [3, 6], applied it to optical fibres. In 1996, Van den Brink [19] defined a master curve in viscoelastic relaxation in using several Maxwell elements (simple exponentials). In 1997, Kannan *et al* [20], use this master curve concept for predictive ends in optical fibres.

As we have already reported in several communications, most of them unpublished [21], the physical assumptions of our approach are the following. The ageing can be described very often by (i) a single one-order physico-chemical reaction (ii) thermally activated for which (iii) the activation energy is distributed according to a distribution function $g(E)$ (iv) independent of the temperature. Then, a simplifying approximation can be used that is called the demarcation energy approximation for computing the relevant physical quantity as a function of time and temperature. A general mathematical procedure is described in [22]. It

is based on the hypotheses (ii)–(iv). This description is phenomenological and is in fact not directly related to the physical processes. For industrial purposes, it works nicely although it describes only one aspect of the problem: the time optimization. For understanding a link between grating elaboration and lifetime, it is necessary to use an analytical approach close to the physical processes. However, this approach suffers from a defect arising from the assumed approximation of demarcation energy. Here, we report a procedure which overcomes some of the restrictions limiting the usefulness of this framework in industrial applications.

For better understanding of the problem, we chose the example of the ageing of the index change induced using the photosensitivity of H_2 loaded germanosilicate core optical fibres. We have shown in a previous publication that a top hat distribution $g(E)$ can be used for modelling the distribution function and for computing the refractive index change $\Delta n(t, T)$ with time t and temperature T [4]. The integration of this distribution gives rise to the following analytical function when using the demarcation energy approximation that simulates the experimental results almost entirely:

$$\Delta n(t,T) = \begin{cases} \Delta n_0 & \text{for } E_\mathrm{d} < E_\mathrm{min} \\ \Delta n_0 \dfrac{E_\mathrm{max} - E_\mathrm{d}}{E_\mathrm{max} - E_\mathrm{min}} & \text{for } E_\mathrm{min} < E_\mathrm{d} < E_\mathrm{max} \\ 0 & \text{for } E_\mathrm{max} < E_\mathrm{d} \end{cases} \tag{1}$$

where $E_\mathrm{d} = k_\mathrm{B} T \ln(k_0 t)$ is the so-called demarcation energy, k_B being the Boltzman constant, Δn_0 is the strength of the index change before ageing, E_min and E_max two energies delimiting the variation of the step-like distribution function, and k_0 the pre-exponential factor of the rate constant of the virtual reaction related to refraction index change relaxation.

E_min, E_max, k_0 are obtained by fitting the experimental database i.e. the set of experimental data measured previously in an accelerated ageing experiment with equation (1) (see figure 1). The problem in this case is that the experiment does not show an angular point at around E_min as it does in the theory. There would be the same observation if we had the data around E_max also. Actually, the experiment is differentiable but not the model. This is not so awkward for the determination of some burning in conditions (although it is not exact). However, this is really a problem for the qualification of device lifetime since the region around the angular point near E_min will be a detrimental factor for the calculation (see figure 1). As a matter of fact, the acceptable decrease of a grating strength over 20–25 years is 1% and this is of the order of the error made using the demarcation energy approximation. What we can see also is that the experimental curve shape according to E_d depends on the annealing temperature which is not included in the model as it can be seen that equation (1) is not depending on T explicitly, though an implicit T dependence comes through E_d. This observation is in fact beyond the approximation of demarcation energy beyond the concept of a master curve [20].

It is thus necessary to correct the defect in this approach and we propose an analytical procedure in this paper for performing more precise estimates applicable to any energy-distributed processes but keeping most of the advantages of the demarcation energy approximation. Our procedure can thus be viewed as a correction to the demarcation energy approximation. In the course of this paper, we will also shed light on a few tricky points about master curve building that are usually ignored.

2. Theory

2.1. The limit of the approximation

The modelling of the stability of the physically relevant quantity, i.e. the refractive index in this paper, is considered proportional to a species B fulfilling the following hypotheses:

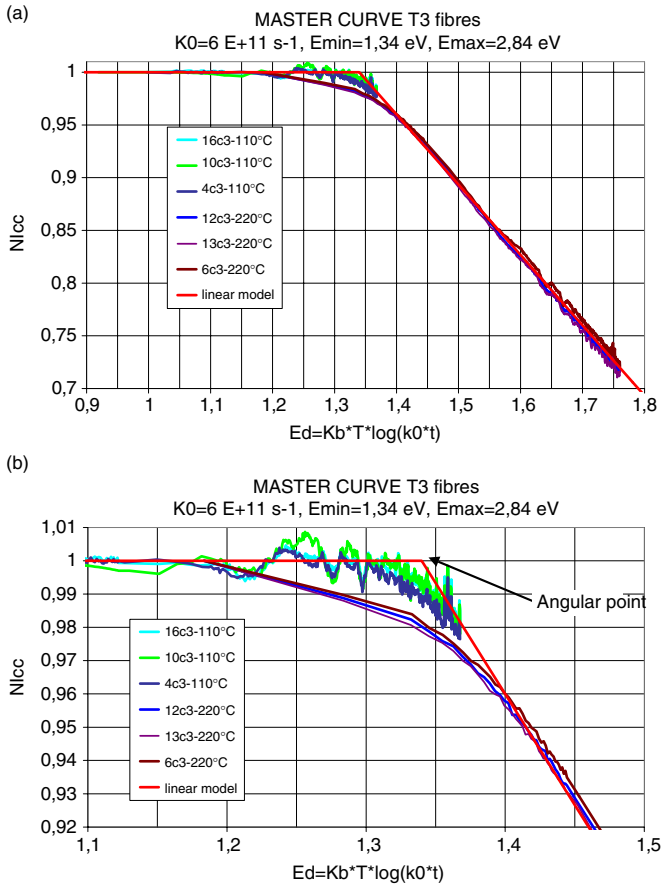

Figure 1. Experimental data set of NICCs (the normalized integrated coupling constant is $\frac{\text{Arc tan}\sqrt{R(t,T)}}{\text{Arc tan}\sqrt{R(t=0)}}$ with R the reflectivity of the grating in consideration, i.e. the normalized refractive index change) plotted against demarcation energy using an optimized k_0 constant in order to obtain, as best as possible, the collapse of the data set, whatever the time t and the temperature T, into only one curve called the master curve. The example considered here is a type of H_2 loaded germanosilicate core optical fibres slightly different from the one used in (4). For this example, $k_0 = 6 \times 10^{11}$ s^{-1}, $E_{\min} = 1.34$ eV, and $E_{\max} = 2.84$ eV. Graph (b) is a magnification of graph (a) around the knee of the curve.

(i) it occurs in a reaction $B \rightarrow A$ that is dominant in a likely complex process,

(ii) this erasing reaction is thermally activated,

(iii) the rate constant of this reaction is $k = k_0 \exp(-E/k_B T)$,

(iv) the activation energy E is distributed according to a distribution function $g(E)$ which is normalized, i.e. $\int_0^\infty g(E)\,\mathrm{d}E = 1$,

(v) the reaction is of first order (although this last condition can be relaxed in some cases).

The quantity B relevant to index change is thus expressed as:

$$B(t,T) = B_0 \int_0^\infty g(E)\eta(t,T,E)\,\mathrm{d}E$$

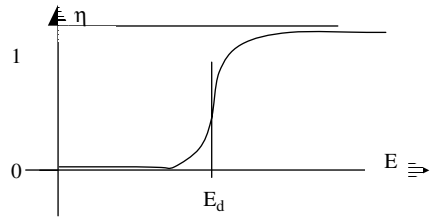

Figure 2. Scheme of decay curve η against the activation energy.

where B_0 is the value of B at $t = 0$, and $\eta(t, T, E)$ is the decay function of the erasure reaction, i.e. the remaining B fraction that can decay through the pathway of activation energy E:

$$\eta(t, T, E) = \exp(-k_0 t \exp(-E/k_B T)).$$

This function is a very steep function of E, commuting from 0 to 1 when E passes through a value E_d called the demarcation energy [21] (see figure 2).

E_d is correctly defined by the position of the inflexion point of η versus E. Thus, it is defined by the following equation [16]:

$$\left.\frac{\partial^2 \eta}{\partial E^2}\right|_{t,T} = 0. \tag{2}$$

For the expression of η here considered, we have $E_d = k_B T \ln(k_0 t)$. Note that E_d has a different expression for second order kinetics or for reversible reactions; see [23], for instance.

We note that for $t = 0$, $E_d = -\infty$, contrary to the activation energy which is always positive. However, $E_d = 0$ for a very small value of t (i.e. $1/k_0$) that can be considered as the initial moment of the ageing.

Then, $B(t, T)$ can be approximated by $b(t, T) = B_0 \int_{E_d}^{\infty} g(E)\,dE = b(E_d)$ taking advantage of the above properties of η.[3] Here, we can note that function b depends only on E_d, that connects to the variables t and T. This is the practical way for analytical computation of $b(E_d)$ which will be fitted afterwards to a experimental $B(t, T)$ data set. From that point, if we differentiate $b(E_d)$, we obtain $\frac{db}{dE_d}(E_d) = -B_0 g(E_d)$ and thus this expression is used for finding $g(E)$ and for calculating the analytical expression of $b(t, T)$, which can be used to fit the experimental data set in the first approximation. But $b(t, T)$ is really very close to $B(t, T)$ only if $|\frac{dg}{dE}| \ll |\frac{\partial \eta}{\partial E}|_{t,T}$ for any E. For instance, this is not at all the case when the energy is not distributed, i.e. when $g(E)$ is equal to a Dirac function $\delta(E - E_0)$ (single reaction pathway). Furthermore, even if g is constant like the case considered in section 1, we have $\frac{B-b}{B_0} = -\gamma g k_B T$ (γ: the Euler constant ≈ 0.577) which is a small[4] but T-dependent term. The

[3] $b(E_d) - B(E_d, T) < \gamma B_0 kT/(E_{max} - E_{min})$ with $\gamma = 0.577$, in the case of a top hat distribution as we will see later in the paper.
Otherwise,

$$\frac{B(E_d, T) - b(E_d)}{B_0} = \int_0^{\infty} g(E)\eta(E_d, T, E)\,dE - \int_{E_d}^{\infty} g(E)\,dE$$
$$= \int_{E_d}^{\infty} g(E)[\eta(E_d, T, E) - 1]\,dE + \int_0^{E_d} g(E)\eta(E_d, T, E)\,dE.$$

The integrands of the two last integrals are localized very closely to E_d and a second order approximation is possible. In particular, if we assume $g(E) = g(E_d)$ on a sufficiently large range around E_d, we have $\frac{B(E_d,T)-b(E_d)}{B_0} = g(E_d)\int_{E_d}^{\infty}[\eta(E_d, T, E) - 1]\,dE + g(E_d)\int_0^{E_d} \eta(E_d, T, E)\,dE$ which is analytically computable and equal to $-\gamma k_B T g(E_d)$.

[4] With our experimental results, $(B - b)/B_0 = -2\% \pm 1\%$, $g = 1/1.5\ \mathrm{eV}^{-1}$, $k_B T(300\ \mathrm{K}) = 1/40\ \mathrm{eV}$.

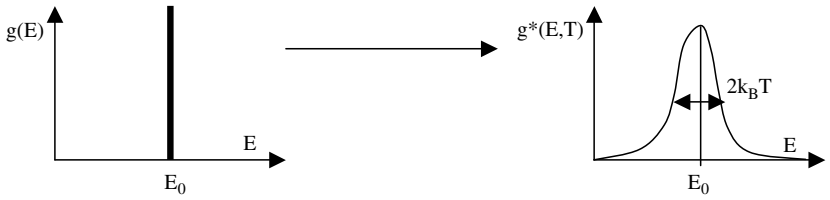

Figure 3. Convolution of Dirac function (the true function) for obtaining the experimental distribution function.

amplitude of the T dependence is of the order of the specification of decrease after 25 years. The appearance of a T dependence is normal because when $b(E_\mathrm{d})$ does not depend on T, B is not only E_d dependent but also T dependent. This is shown in the next section.

The problem having been expressed, we now describe below a procedure for correcting the error introduced in the demarcation energy approximation while preserving most of the advantages of this approximation.

2.2. To overcome the approximation limitation: definition of the experimental activation energy distribution function

Despite the problem described above, we can differentiate $B(t, T)$ versus E_d. Let us note for this purpose that $\eta(t, T, E) = \exp(-k_0 t \exp(-E/k_\mathrm{B}T))$, replacing t by its expression as a function of E_d as defined from equation (2), we get

$$\eta(t, T, E) = \eta(E_\mathrm{d}, T, E) = \exp(-\exp((E_\mathrm{d} - E)/k_\mathrm{B}T)) = \eta^*(E_\mathrm{d} - E, T)$$

where $\eta^*(E^*, T)$ is the formal function $\exp(-\exp(E^*/k_\mathrm{B}T))$ with E^* a symbolic variable. We have:

$$B(t, T) = B(E_\mathrm{d}, T) = B_0 \int_0^\infty g(E)\eta^*(E_\mathrm{d} - E, T)\,\mathrm{d}E.$$

Here, we note that $B(E_\mathrm{d}, T)$ is the convolution of $g(E^*)$ with $\eta^*(E^*, T)$ with E^* a symbolic variable assuming that $g(E) = 0$ for $E < 2k_\mathrm{B}T$. The differentiation leads therefore to:

$$\left.\frac{\partial B}{\partial E_\mathrm{d}}\right|_T (E_\mathrm{d}, T) = B_0 \int_0^\infty g(E) \left.\frac{\partial \eta^*}{\partial E^*}\right|_T (E_\mathrm{d} - E, T)\,\mathrm{d}E = B_0 \left(g^* \left.\frac{\partial \eta^*}{\partial E^*}\right|_T \right)(E_\mathrm{d}, T).$$

By analogy with $\mathrm{d}b/\mathrm{d}E_\mathrm{d}$, we can see that the partial differentiation of experimental data set (B) at constant T results in an experimental distribution $g^*(E, T) = -\left(g^* \left.\frac{\partial \eta^*}{\partial E^*}\right|_T\right)(E, T)$, i.e. the true distribution g convoluted by $-\left.\frac{\partial \eta^*}{\partial E^*}\right|_T$.

For example, if one considers $g(E) = \delta(E - E_0)$ (unique activation energy or single reaction pathway), the experimental distribution $g^*(E, T)$ will be

$$g^*(E, T) = -\left.\frac{\partial \eta^*}{\partial E^*}\right|_T (E - E_0, T) = \eta^*(E - E_0, T)\frac{1}{k_\mathrm{B}T}\exp\left(\frac{E - E_0}{k_\mathrm{B}T}\right) \tag{3}$$

i.e. an asymmetrical bell shaped curve with a width of $\approx 2k_\mathrm{B}T$ (see figure 3).

Important note: we remark here that $-\left.\frac{\partial \eta^*}{\partial E^*}\right|_T$ is not only a function of E^* but also of T. $g^*(E, T)$ is therefore also dependent on T. This stands therefore beyond the master curve approach. Note that if $g(E)$ is the physical distribution which yields $B(E_\mathrm{d}, T)$ after exact integration, $g^*(E, T)$ is a corrected distribution which allows using the demarcation energy approximation.

As a matter of fact, reciprocally, for computing an analytical expression for $B(E_\mathrm{d}, T)$ (let us call it $\tilde{B}(E_\mathrm{d}, T)$), we would like to use the demarcation energy method knowing $g^*(E, T)$. We have to note that

$$\begin{aligned}\int_{E_\mathrm{d}}^{\infty} g^*(E,T)\,\mathrm{d}E &= \int_{E_\mathrm{d}}^{\infty} -\left(g^*\frac{\partial\eta^*}{\partial E^*}\bigg|_T\right)(E,T)\,\mathrm{d}E \\ &= \int_{E_\mathrm{d}}^{\infty}\mathrm{d}E\int_0^{\infty} -g(E')\frac{\partial\eta^*}{\partial E^*}\bigg|_T(E_\mathrm{d}-E',T)\,\mathrm{d}E' \\ &= \int_0^{\infty}\mathrm{d}E'\,g(E')\underbrace{\int_{E_\mathrm{d}-E'}^{\infty} -\frac{\partial\eta^*}{\partial E^*}\bigg|_T(E^*,T)\,\mathrm{d}E^*}_{=-\eta^*(\infty,T)+\eta^*(E_\mathrm{d}-E',T)} \\ &= \int_0^{\infty} g(E')\eta^*(E_\mathrm{d}-E',T)\,\mathrm{d}E' - \underbrace{\int_0^{\infty} g(E')\eta^*(\infty,T)\,\mathrm{d}E'}_{=0\quad\text{because}\quad\eta^*(\infty,T)=0} = \frac{B(E_\mathrm{d},T)}{B_0}.\end{aligned}$$

It is worth noting that we can obtain in such a way a theoretical expression $\tilde{B}$ for the experimental data set B if $g^*(E, T)$ deduced from the differentiation of the data set has been analytically modelled.

In particular, considering $g(E) = \delta(E - E_0)$ we deduce using equation (3) the following:

$$\tilde{B}(E_\mathrm{d}, T) = B_0\int_{E_\mathrm{d}}^{\infty} g^*(E,T)\,\mathrm{d}E$$

and thus

$$\begin{aligned}B_0\int_{E_\mathrm{d}}^{\infty} -\frac{\partial\eta^*}{\partial E^*}\bigg|_T(E-E_0,T)\,\mathrm{d}E &= B_0\eta^*(E_\mathrm{d}-E_0,T) \\ &= B_0\int_0^{\infty}\delta(E-E_0)\eta^*(E_\mathrm{d}-E,T)\,\mathrm{d}E)\end{aligned}$$

which is exactly the expression of $B(E_\mathrm{d}, T)$.

We conclude therefore that the use of $g^*(E, T)$ extends the validity of the demarcation energy method to any kind of distribution providing that it does not approach $E = 0$ close to $2k_\mathrm{B}T$.

3. Application

The method that we suggest using is the following. It runs in four steps.

(1) Application of demarcation energy approximation to the experimental data set $B(E_\mathrm{d}, T)$. We get a master curve with some remaining T dependence and then the experimental distribution $g^*(E, T)$.
(2) A physical distribution $g(E)$ can be deduced from $g^*(E, T) = -\left(g^*\frac{\partial\eta^*}{\partial E^*}\big|_T\right)(E, T)$.
(3) The modelling of g^* gives rise by analytical integration to analytical $\tilde{B}(E_\mathrm{d}, T)$ and the modelling of $g(E)$ gives rise to $b(E_\mathrm{d})$, both containing adjustable parameters.
(4) Adjustable parameters are fixed by fitting the experimental data set $B(E_\mathrm{d}, T)$ with $\tilde{B}(E_\mathrm{d}, T)$ or with $b(E_\mathrm{d})$.

Here is an example of the application of this procedure to the case of the stability of a Bragg grating written in a H_2 loaded Ge doped silica core optical fibre.

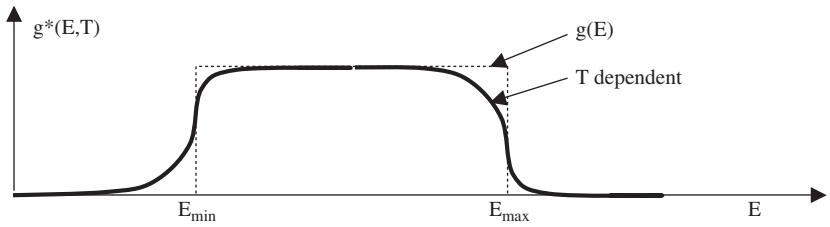

Figure 4. The experimental distribution function $g^*(E, T)$ conjugated to the top-hat function $g(E)$. Note the disymmetry at the edges.

Step 1. In the case mentioned above, the distribution function is suggested to be a top hat, like the following:

$$g(E) = \begin{cases} 0 & \text{for } E < E_{\min} \\ \dfrac{1}{E_{\max} - E_{\min}} & \text{for } E_{\min} < E < E_{\max} \\ 0 & \text{for } E_{\max} < E \end{cases}$$

where $E_{\min}$, $E_{\max}$ are the lower and higher bound of the function, respectively (see figure 4).

Step 2. The experimental distribution is then:

$$\begin{aligned} g^*(E, T) &= \int_0^\infty -g(E') \frac{\partial \eta^*}{\partial E^*}\bigg|_T (E - E', T)\, \mathrm{d}E' \\ &= -\int_{E_{\min}}^{E_{\max}} \frac{1}{E_{\max} - E_{\min}} \frac{\partial \eta^*}{\partial E^*}\bigg|_T (E - E', T)\, \mathrm{d}E' \\ &= \frac{1}{E_{\max} - E_{\min}} (\eta^*(E - E_{\min}, T) - \eta^*(E - E_{\max}, T)). \end{aligned}$$

This is shown in figure 4.

Step 3. Let us compute $\tilde{B}(E_{\mathrm{d}}, T)$ now; we have:

$$\begin{aligned} \tilde{B}(E_{\mathrm{d}}, T) &= B_0 \int_{E_{\mathrm{d}}}^\infty g^*(E, T)\, \mathrm{d}E \\ &= \frac{B_0}{E_{\max} - E_{\min}} \left(\int_{E_{\mathrm{d}}}^\infty \eta^*(E - E_{\min}, T)\, \mathrm{d}E - \int_{E_{\mathrm{d}}}^\infty \eta^*(E - E_{\max}, T)\, \mathrm{d}E \right) \\ &= B_0 \frac{I_{\max}(E_{\mathrm{d}}, T) - I_{\min}(E_{\mathrm{d}}, T)}{E_{\max} - E_{\min}} \\ I_{\min}(E_{\mathrm{d}}, T) &= \int_{E_{\mathrm{d}}}^\infty \exp\left(-\exp\left(\frac{E - E_{\min}}{k_{\mathrm{B}} T} \right) \right) \mathrm{d}E. \end{aligned}$$

Making the following variable change:

$$y = \exp\left(\frac{E - E_{\min}}{k_{\mathrm{B}} T} \right),$$

we get:

$$I_{\min}(E_{\mathrm{d}}, T) = k_{\mathrm{B}} T \int_{\exp(\frac{E_{\mathrm{d}} - E_{\min}}{k_{\mathrm{B}} T})}^\infty \frac{\exp(-y)}{y}\, \mathrm{d}y = k_{\mathrm{B}} T\, E_1 \left(\exp\left(\frac{E_{\mathrm{d}} - E_{\min}}{k_{\mathrm{B}} T} \right) \right)$$

where E_1 is the Euler integral.

So, $\tilde{B}(E_\mathrm{d}, T)$ is thus:

$$\tilde{B}(E_\mathrm{d}, T) = \frac{B_0 k_\mathrm{B} T}{E_\mathrm{max} - E_\mathrm{min}} \left[E_1\left(\exp\left(\frac{E_\mathrm{d} - E_\mathrm{max}}{k_\mathrm{B} T}\right)\right) - E_1\left(\exp\left(\frac{E_\mathrm{d} - E_\mathrm{min}}{k_\mathrm{B} T}\right)\right)\right]$$
$$= \frac{B_0 k_\mathrm{B} T}{E_\mathrm{max} - E_\mathrm{min}} I(E_\mathrm{d}, T).$$

The difference $I(E_\mathrm{d}, T)$ can be reorganized using the series expansion [24]

$$E_1(x) = -\gamma - \ln(x) - \sum_{n=1}^{\infty} (-1)^n \frac{x^n}{n.n!}$$

where γ is the Euler constant[5].

We get:

$$I(E_\mathrm{d}, T) = \frac{E_\mathrm{max} - E_\mathrm{min}}{k_\mathrm{B} T} + \sum_{n=1}^{\infty} \frac{(-1)^n}{n.n!} \exp\left(\frac{n E_\mathrm{d}}{k_\mathrm{B} T}\right) \left[\exp\left(-\frac{E_\mathrm{min}}{k_\mathrm{B} T}\right) - \exp\left(-\frac{E_\mathrm{max}}{k_\mathrm{B} T}\right)\right]^n.$$

Therefore

$$\tilde{B}(E_\mathrm{d}, T)/B_0 = 1 + \frac{k_\mathrm{B} T}{E_\mathrm{max} - E_\mathrm{min}} \sum_{n=1}^{\infty} \frac{(-1)^n}{n.n!} \exp\left(\frac{n E_\mathrm{d}}{k_\mathrm{B} T}\right) \left[\exp\left(-\frac{E_\mathrm{min}}{k_\mathrm{B} T}\right) - \exp\left(-\frac{E_\mathrm{max}}{k_\mathrm{B} T}\right)\right]^n.$$

Let us study the behaviour of $B(E_\mathrm{d}, T)$ around E_min now, and for that purpose let us state $E_\mathrm{d} = E_\mathrm{min} + \delta E$; we get:

$$\tilde{B}(E_\mathrm{d}, T)/B_0 = 1 + \frac{k_\mathrm{B} T}{E_\mathrm{max} - E_\mathrm{min}} \sum_{n=1}^{\infty} \frac{(-1)^n}{n.n!} \exp\left(\frac{n \delta E}{k_\mathrm{B} T}\right) \left[1 - \exp\left(-\frac{E_\mathrm{max} - E_\mathrm{min}}{k_\mathrm{B} T}\right)\right]^n.$$

But in our case

$$\frac{E_\mathrm{max} - E_\mathrm{min}}{k_\mathrm{B} T} \gg 1 \Rightarrow \exp\left(-\frac{E_\mathrm{max} - E_\mathrm{min}}{k_\mathrm{B} T}\right) \ll 1$$

and so:

$$\tilde{B}(E_\mathrm{d}, T)/B_0 = 1 + \frac{k_\mathrm{B} T}{E_\mathrm{max} - E_\mathrm{min}} \sum_{n=1}^{\infty} \frac{(-1)^n}{n.n!} \exp\left(\frac{n \delta E}{k_\mathrm{B} T}\right). \tag{4}$$

When $\delta E < 0$, $\exp(\frac{\delta E}{k_\mathrm{B} T})^n \to_{n\to\infty} 0$ and so $\tilde{B}(E_\mathrm{d}, T)/B_0 \to 1$ when δE departs from 0 on the negative side. Computation shows that this is achieved in a few $k_\mathrm{B} T$ and for a moderate number of terms (see figure 5): less than eight.

When $\delta E = 0$, $\sum_{n=1}^{\infty} \frac{(-1)^n}{n.n!} = -E_1(-1) - \gamma = -0.804 < 0$ and thus $\frac{\tilde{B}(E_\mathrm{min}, T)}{T B_0} = 1 - 0.804 \frac{k_\mathrm{B} T}{E_\mathrm{max} - E_\mathrm{min}}$.

However, when $\delta E > 0$, the convergence is different and another approximation has to be used. As we can see in figure 1, the curve $B(E_\mathrm{d}, T)/B_0$ approaches a straight line with equation $1 - \frac{E_\mathrm{d} - E_\mathrm{min}}{E_\mathrm{max} - E_\mathrm{min}} = \frac{E_\mathrm{max} - E_\mathrm{d}}{E_\mathrm{max} - E_\mathrm{min}}$. Here, the quantity E_d that we can call the experimental demarcation energy contains a k_0 term fitted on the data.

However, when we compute the difference between $\frac{\tilde{B}(E_\mathrm{d}, T)}{B_0}$ and $\frac{b(E_\mathrm{d})}{B_0} = \frac{E_\mathrm{max} - E_\mathrm{d}}{E_\mathrm{max} - E_\mathrm{min}}$, we find not zero for $\delta E > 0$ but something slightly different. We have

$$\frac{\tilde{B}(E_\mathrm{d}, T)}{B_0} - \frac{E_\mathrm{max} - E_\mathrm{d}}{E_\mathrm{max} - E_\mathrm{min}} = \frac{\delta E}{E_\mathrm{max} - E_\mathrm{min}} + \frac{k_\mathrm{B} T}{E_\mathrm{max} - E_\mathrm{min}} \sum_{n=1}^{\infty} \frac{(-1)^n}{n.n!} \exp\left(\frac{n \delta E}{k_\mathrm{B} T}\right)$$

[5] $\gamma = 0.577$, $E_1(1) = 0.227$, $E_1(x) \longrightarrow_{x\to 0} -\ln(x) - \gamma$, $E_1(x) \longrightarrow_{x\to+\infty} 0$.

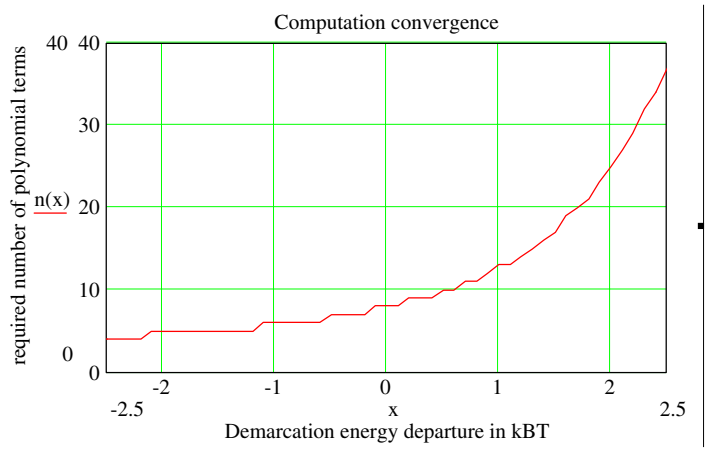

Figure 5. Number of terms required for a precision of 10^{-4} in the normalized B concentration calculation.

or

$$\frac{\tilde{B}(E_\mathrm{d},T)}{B_0}-\frac{E_\mathrm{max}-E_\mathrm{d}}{E_\mathrm{max}-E_\mathrm{min}}=\frac{k_\mathrm{B}T}{E_\mathrm{max}-E_\mathrm{min}}\left(\frac{\delta E}{k_\mathrm{B}T}+\sum_{n=1}^{\infty}\frac{(-1)^n}{n.n!}\exp\left(\frac{n\delta E}{k_\mathrm{B}T}\right)\right)$$
$$=-\frac{k_\mathrm{B}T}{E_\mathrm{max}-E_\mathrm{min}}\left(\gamma+E_1\left(\exp\left(\frac{\delta E}{k_\mathrm{B}T}\right)\right)\right)\underset{\delta E>k_\mathrm{B}T}{\longrightarrow}-\gamma\frac{k_\mathrm{B}T}{E_\mathrm{max}-E_\mathrm{min}}.$$

This discrepancy is rather small, i.e. about 5×10^{-3} per 100 K, but it is T dependent. $\tilde{B}(E_\mathrm{d},T)$ tends therefore to a temperature-dependent function of demarcation energy E_d. This means that the isotherms are no longer coincident as is exemplified in [25] and isochrons are no longer linear curves as in the crude model. However, in our particular case, this discrepancy can be integrated in k_0. This induces a change of theoretical k_0 into $k_0\exp(\gamma)$, i.e. a multiplication by 1.78. Therefore, it is better to change the variable from E_d to $E'_\mathrm{d}=E_\mathrm{d}+\gamma k_\mathrm{B}T=k_\mathrm{B}T\ln(\exp(\gamma)k_0t)$ already in $\tilde{B}$ and to plot the data B versus E'_d in order to minimize the effect of T and to stay as closer as possible to the master curve approximation. From an analytical point of view, this does not change anything in the analysis procedure and the experimental data can still be fitted with the same type of function but the theoretical k_0 is 1.78 times smaller.

More important is the curve knee approximation. We can see in figure 6 that the limited series we have used converges rapidly in one $k_\mathrm{B}T$ on the positive side of the activation energy departure from E_min. At this demarcation energy departure, we find in figure 5 that 13 terms are necessary for a precision of 10^{-4}. Therefore, the practical expression to use for $\tilde{B}(E_\mathrm{d},T)$ is:

$$\tilde{B}(E_\mathrm{d},T)/B_0=1+\frac{k_\mathrm{B}T}{E_\mathrm{max}-E_\mathrm{min}}\sum_{n=1}^{13}\frac{(-1)^n}{n.n!}\exp\left(\frac{n(E_\mathrm{d}-E_\mathrm{min})}{k_\mathrm{B}T}\right).\qquad(5)$$

This can be computed rapidly with any software (we did it with the help of Mathcad© software; the calculation time is less than one second). For demarcation energy above $E_\mathrm{min}+k_\mathrm{B}T$, the classical expression has to be used, i.e. $\frac{b(E'_\mathrm{d})}{B_0}=\frac{E_\mathrm{max}-E'_\mathrm{d}}{E_\mathrm{max}-E_\mathrm{min}}$ with $E'_\mathrm{d}=k_\mathrm{B}T\ln(\exp(\gamma)k_0t)=E_\mathrm{d}+\gamma k_\mathrm{B}T$.

In addition, for sake of programming simplicity, it is possible to use the expression (5) for the negative side and to consider the function equal to 1 for $E_\mathrm{d}<E_\mathrm{min}-4k_\mathrm{B}T$.

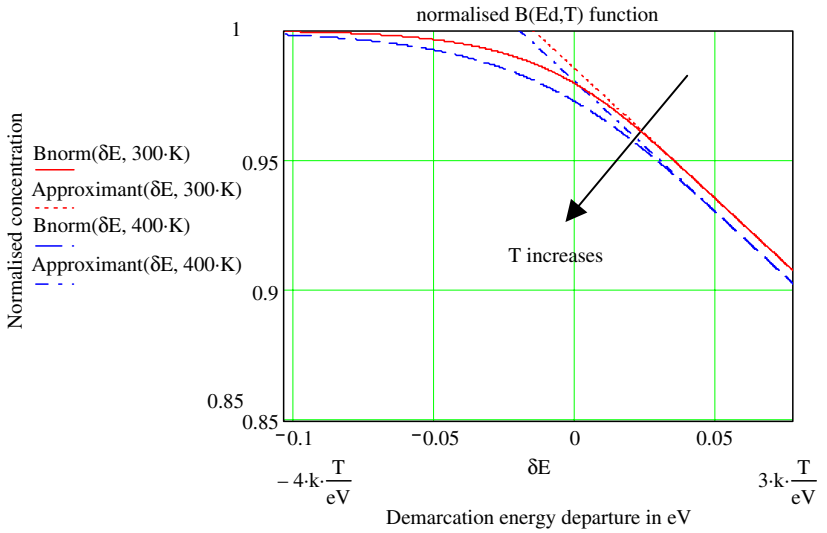

Figure 6. Plot of $\tilde{B}(E_\mathrm{d}, T)/B_0$ called here Bnorm and plot of $\frac{b(E_\mathrm{d})}{B_0} - \gamma \frac{k_\mathrm{B}T}{E_\mathrm{max}-E_\mathrm{min}}$ called here Approximant.

Finally, we notice that, in using E'_d, the linear part appears to be independent but not the knee, which is more softened as the temperature increases.

Step 4. Finally, we have fitted k_0, E_min and E_max on the data set shown in figure 1 and we have found the same values as before but this time with an additional factor 1.78 corresponding to $\exp(\gamma)$. From that result, we plotted the simulation for comparison (figure 7). We now have a curve for activation energy located around E_min that it is similar to the experimental results.

4. Discussion

4.1. Lifetime calculation after elaboration

Now, we have a more precise stability function for fitting our data and performing lifetime prediction after elaboration. For the discussion here, we consider that the physical distribution is a top-hat function at the end of the writing process. The first knee on the curve is thus softened only by the nonzero temperature of the work specification. We can discuss the error we made before, using the linear approximation with the unconvoluted top-hat function.

When one wishes to make an estimate of lifetime for a relative decrease ε, i.e. $1 - B/B_0$ after a time t at T_w (work temperature) defined by $\frac{B(t,T_\mathrm{w})}{B_0} = 1 - \varepsilon$, there are two cases. If ε is large enough such that $\frac{B(t,T_\mathrm{w})}{B_0}$ falls at *position 1* in figure 8 with lifetime t_1, there is no error because B/B_0 follows the linear behaviour for which the correction (as shown above) has no effect and the simplest theory is applicable. However, if ε is small, it falls at *position 2* in figure 8 with lifetime t_2 according to the crude theory, instead of being at *position 3* with lifetime t_3. The lifetime is thus overestimated. The overestimate is obtained by solving the following set of equations:

$$\frac{B}{B_0}(t_3, T_\mathrm{w}) = 1 - \varepsilon = \frac{b(t_2, T_\mathrm{w})}{B_0}.$$

The error (of the order of 2×10^{-2} eV) corresponds to $k_\mathrm{B}T(\ln(t_3) - \ln(t_2))$ and thus to a time reduction factor of about 2 at room temperature. The lifetime has thus been overestimated by twice its actual value.

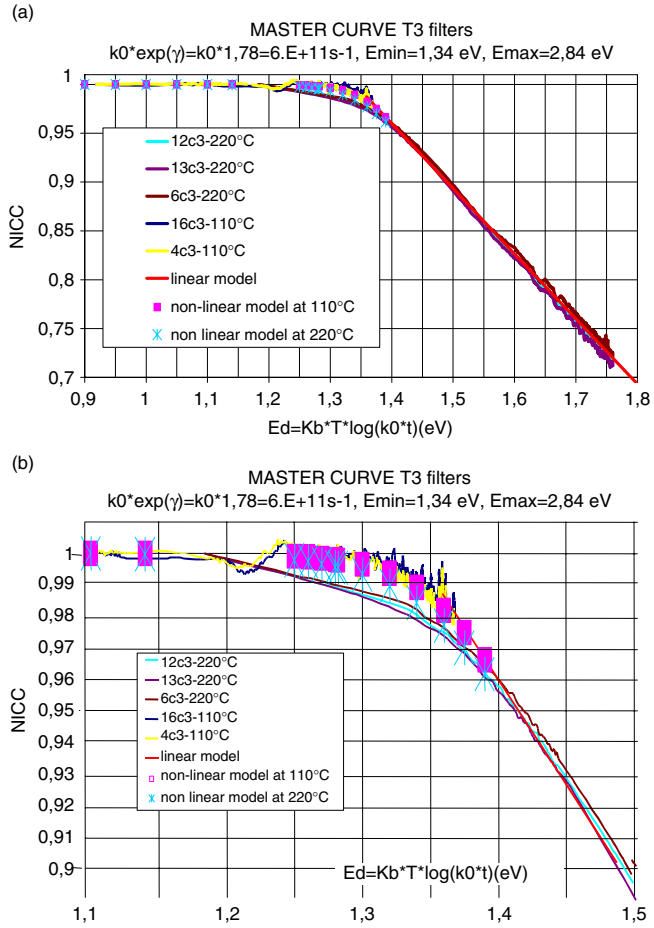

Figure 7. Experimental data set fitted with the new approximation taking into account the small temperature dependence (a). The nonlinear model is marked with crosses and squares. (b) A magnification of (a).

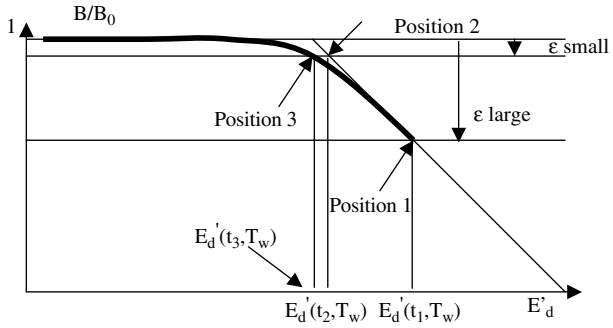

Figure 8. Positions of the grating strength according to the different treatments or specifications.

4.2. Lifetime mastering, determination of burning in

For mastering the lifetime in distributed activation energy systems, a method consists in performing accelerated ageing. In such a way, the less stable part of the system is erased.

The annealing is adjusted in order to obtain a remaining part of the system that is stable for the specified period. For calculating properly the annealing duration, we have to take into account that the distribution function is changed by the annealing treatment at temperature T_a during a time t_a. We will call the B and b functions after annealing B_1 and b_1. They are related to the new stability curve of the system according to the time set to 0 just after the end of the annealing period.

The equations for following the evolution beyond the end of the annealing and beginning of ageing afterwards are:

$$\frac{B_1(0, T_w)}{B_0} = \frac{B(t_{eq}, T_w)}{B_0} = \frac{B(t_a, T_a)}{B_0}$$

where t_{eq} is an equivalent time at T_w corresponding to a decay achieved at T_a during t_a. For fixing the lifetime t_1 at T_w according to the annealing parameters (t_a, T_a), we have to solve the following equation:

$$\frac{B_1(t_1, T_w)}{B_0} = (1 - \varepsilon)\frac{B_1(0, T_w)}{B_0}. \tag{6}$$

This translates a decay of amplitude ε of the system after burning in.

Using the $b(E_d)$ approach. For the stepwise distribution and for the crude model, the corresponding equations above are obtained just by replacing B by b. We get:

$$\frac{b_1(0, T_w)}{B_0} = \frac{b(t_{eq}, T_w)}{B_0} = \frac{b(t_a, T_a)}{B_0} \quad \text{and} \quad \frac{b_1(t_1, T_w)}{B_0} = (1 - \varepsilon)\frac{b_1(0, T_w)}{B_0}$$

$$\frac{b_1(E'_d)}{b_1(0)} = \begin{cases} 1 & \text{for } E'_d < k_B T_a \ln[\exp(\gamma) k_0 t_a] \\ \dfrac{E_{max} - E'_d}{E_{max} - k_B T_a \ln[\exp(\gamma) k_0 t_a]} & \text{for } k_B T_a \ln[\exp(\gamma) k_0 t_a] < E'_d < E_{max} \\ 0 & \text{for } E_{max} < E'_d \end{cases}$$

$$\text{with } E'_d = k_B T \ln(k_0 t \exp(\gamma))$$

$b_1(E'_d)$ is obtained

(i) by changing E_{min}, into $k_B T_a \ln[\exp(\gamma) k_0 t_a]$ in $b(E'_d)$ as the annealing has removed the less stable sites of the distribution, and

(ii) by renormalizing by $b_1(0)$.

The time t_{eq} is a much longer period of time at T_w corresponding to the annealing during t_a at T_a. It is obtained here by $E'_d(t_a, T_a) = E'_d(t_{eq}, T_w)$ as function b depends only on E'_d (see figure 9).

Then, after annealing, the lifetime for a further decrease in b/B_0 of ε should be computed at T_w again. This, however, is a straightforward task after t_{eq} determination by solving the equation for b_1.

Once the annealing is done, one wants to cross check if the measured lifetime is actually what has been computed. At that time usually, just after the burning in, the time scale is set again to zero and a new master curve is plotted. We have to be aware that this time scale shift modifies the stability curve.

Its shape is obtained by setting the time to zero after annealing at the beginning of the ageing experiment and in plotting $b_1(t_1, T_w)/b_1(0, T_w)$ according to the new demarcation energy $E''_d = k_B T_w \ln(\exp(\gamma) k_0 t_1)$, where t_1 is the new time scale with $t_1 = t - t_{eq}$ as in figure 9. The $b_1(t_1, T_w)/b_1(0, T_w)$ function will be thus transformed into:

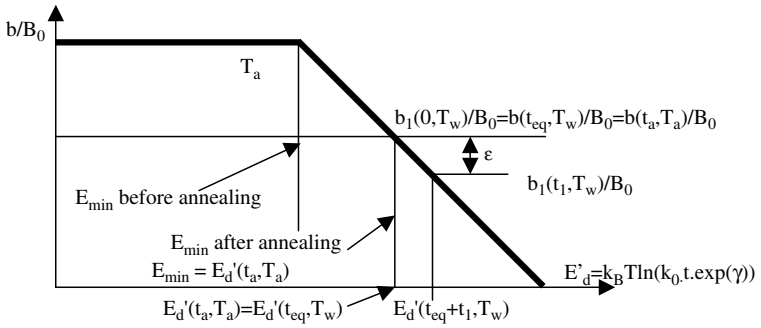

Figure 9. Lifetime estimate after an annealing treatment using the master curve before annealing in the case of the crude model.

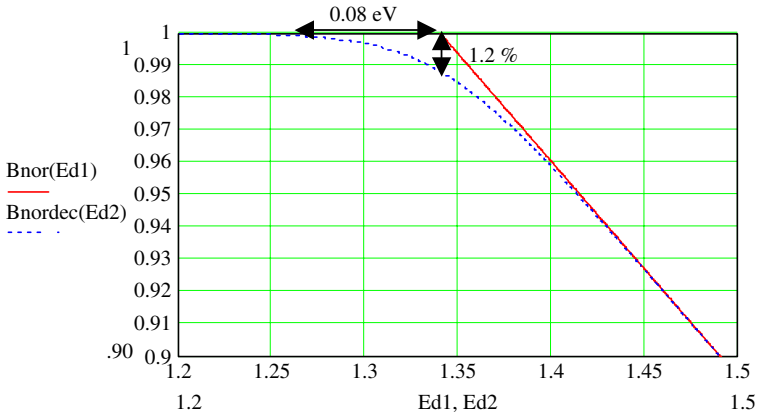

Figure 10. Plot of $b_1(E'_d)/b_1(0, T_w)$ called on the graph Bnor($Ed1$), and of $b_1(E''_d)/b_1(0, T_w)$ called on the graph Bnordec($Ed2$). We can see that the change of the time origin leads to a curve exhibiting again a softened knee.

$$\frac{b_1(E'_d)}{b_1(0,T_w)} = \frac{b_1(k_B T_w \ln(\exp(\gamma)k_0 t))}{b_1(0,T_w)} = \frac{b_1(k_B T_w \ln(\exp(\gamma)k_0(t_1+t_{eq})))}{b_1(0,T_w)}$$
$$= \frac{b_1\left(k_B T_w \ln\left(\exp\left(\frac{E''_d}{k_B T_w}\right) + \exp(\gamma)k_0 t_w\right)\right)}{b_1(0,T_w)} = \frac{b_1(E''_d)}{b_1(0,T_w)}.$$

The result is plotted in figure 10.

For $t_1 \ll t_{eq}$, the change of b_1 value is small, but not for $t_1 \approx t_{eq}$. For $t_1 \gg t_{eq}$, the change is also negligible. We can notice that the time shift itself introduces a smoothing of the curve but this one is not T_w dependent, contrary to the previous one. Therefore, within the crude model, the stability curve is easily obtained; it is smoothed but independent of the work temperature. The magnitude of the decrease is of 1.2% at the maximum.

If we check the lifetime on $b_1(E''_d)$ (by determining the time for an ε decrease), we will see that the *demarcation energy value* is different from the one predicted with $b_1(E'_d)$ but both energies correspond in fact to the same *time* as for the prediction we used E'_d and for checking we use E''_d containing a time shift. The calculation is thus consistent.

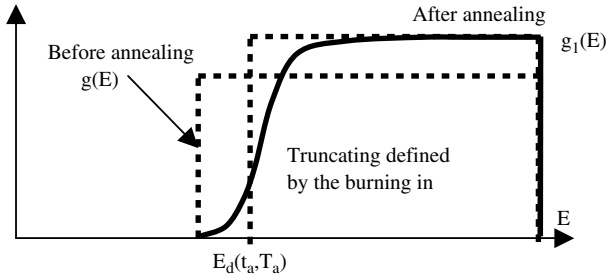

Figure 11. Effect of the annealing on the activation energy distribution function.

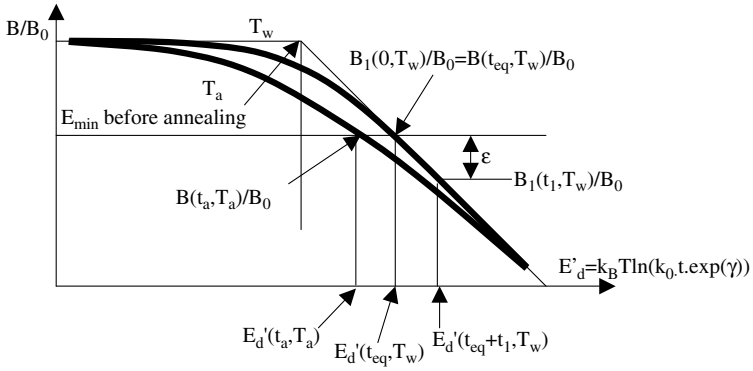

Figure 12. Lifetime estimate after an annealing treatment using the master curve before annealing in the case of the corrected model.

In using $B(E_\mathrm{d}, T)$ approach. The function $B_1(t_1, T_\mathrm{w})$ or $b_1(t_1, T_\mathrm{w})$ is based on the distribution function $g(E)$ modified by the annealing treatment: $g_1(E)$ in figure 11. In the case of crude theory, the distribution after annealing is just the distribution function before annealing truncated at the demarcation energy reached at the end of the annealing treatment and renormalized. In the correct theory, the distribution function $g(E)$ is modified on its lower edge by the effect of the annealing (figure 11). Its expression is:

$$g_1(E) = \frac{g(E)\eta(t_\mathrm{a}, T_\mathrm{a}, E)}{\int_0^\infty g(E)\eta(t_\mathrm{a}, T_\mathrm{a}, E)\,\mathrm{d}E}.$$

Now, this new distribution function will be 'read' at a temperature T_w, the work temperature. The new practical distribution is thus obtained by convolution of the 'annealed' distribution by the derivation of the decay function $-\frac{\partial \eta^*}{\partial E^*}\big|_T$ as described in section 2. The effect, nevertheless, is here, *a priori*, more complex than after grating elaboration and has to be addressed.

Let us start as before with the stability curves according to E'_d. We can assume that the temperature T_w is significantly lower than T_a and thus that the smoothing introduced by the convolution at T_w is smaller than the one at T_a. Figure 12 is drawn with this assumption.

The burning in at T_a during time t_a decreases B/B_0 from 1 to $B(t_\mathrm{a}, T_\mathrm{a})/B_0$. Then, we have to commute to the isotherm at T_w for considering a further ageing during lifetime t_1 at this temperature. One difference with the crude case is that now $E'_\mathrm{d}(t_\mathrm{a}, T_\mathrm{a}) \neq E'_\mathrm{d}(t_\mathrm{eq}, T_\mathrm{w})$. Nevertheless, the procedure remains the same although the equations are a bit more complicated.

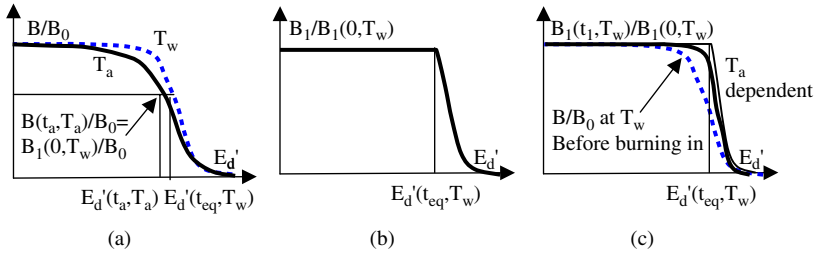

Figure 13. Construction of the new stability curve after annealing. (a) Reduction of B due to the annealing at T_a during t_a (continuous line) and commutation on T_w curve (dashed line). (b) Truncated T_w curve after renormalization without considering the smoothing introduced by the annealing. (c) Real curve (thick continuous line) plotted against old demarcation energy E'_d compared to the stability curve before burning in. The thin line is curve (b).

So, we have performed the annealing and we want to check the predicted lifetime. At this stage, we have to consider that the distribution function is no longer $g(E)$ but $g_1(E)$, as noted above, and that we will measure the stability curve by 'reading' at a higher temperature than the work temperature (accelerated ageing as for the first determination of the stability curve). Finally, the shape of this curve will be defined both by the annealing temperature T_a and by the temperature of reading. If we consider the work temperature that is always lower than T_a, the condition $|\frac{dg_1}{dE}| \ll |\frac{\partial \eta}{\partial E}|_{t,T_w}$ is fulfilled and the effect of the convolution will be almost negligible. The stability curve will be thus only defined by the burning in temperature.

Figure 13 shows how to build the new stability curve. The position $E'_d(t_a, T_a)$ in figure 13(a) shows the point reached by the grating at the end of an annealing. Then, the grating is cooled down and will be used at T_w. We can thus truncate the T_w stability curve at $E'_d(t_{eq}, T_w)$ and renormalize by the B value at the end of the annealing (figure 13(b)). Then, we have to take into account the smoothing introduced by $\eta(t_a, T_a, E)$ (see figure 11).

As can be seen in figure 13(c), the difference between the predicted lifetime from figure 12 or 13(a) and the real one is similar to the one described in figure 8: the real lifetime is shorter than the one predicted by simple application of the demarcation energy approximation. This result is due to the fact that the cutting of $g(E)$ is not abrupt (see figure 11). There remains thus some sites below $E'_d(t_a, T_a)$. Calculations show that the predicted lifetime is twice as small as the actual lifetime for a decrease of 1%. Knowing this, it is easy to correct the burning in parameters.

4.3. Time shift with corrected model

In the corrected model, the effect of time shift in the B_1 function leads to the same effect as with b_1. This results in a knee on the curve which is relatively more softened but without any change in the lifetime.

5. Conclusion

In this paper, we have developed a correction to the demarcation energy approximation for improving the prediction of the lifetime of devices. The correction is based on a convolution of the physical distribution with a function that introduces back a temperature dependence left aside by the demarcation energy approximation. This procedure is advantageous only in the region of the stability curve where the variation of the distribution function is steep, especially

around the angular points. In the constant or weakly changing slope region of the distribution function, the crude formula, being more simple, should be used.

The correction procedure we describe here shows that it is possible to use the demarcation energy approximation and its interesting features such as time–temperature equivalence or analytic integration of classical distribution functions, except when $|\frac{\mathrm{d}g}{\mathrm{d}E}| \ll |\frac{\partial \eta}{\partial E}|_{t,T}$. When this latter is true, it is worthwhile performing the correction by the procedure described in this paper. This is the case especially for lifetime certification of a Bragg grating written in hydrogen loaded germanosilicate core optical fibres as the certification of a decrease of less than 1% during the lifetime falls in the critical region. Our analysis shows that neglecting the limit of the demarcation energy approximation leads to an overestimate of the lifetime by a factor of about 2.

Finally, we emphasize that the procedure described in this paper is applicable to other systems as well for which the activation energy is distributed. There is no restriction to optics or to a given distribution function.

Acknowledgment

We are very grateful to T Lafforgue for his help with the mathematical formulation of this work.

References

[1] Richert R and Blumen A (ed) 1994 *Disorder Effects on Relaxational Processes* (Berlin: Springer)
[2] Bernage P *et al* 1996 Inscription kinetics and thermal stability of Bragg gratings written within heated fibers *Doped Fiber Devices and Systems II* (Denver, CO: SPIE) pp 70–83
[3] Erdogan T, Mizrahi V, Lemaire P J and Monroe D 1994 Decay of U.V.-induced fiber Bragg gratings *Optical Fiber Communication'94 (Washington, DC, USA)* ed OSA (San Jose, CA: Optical Society of America) p 50
[4] Riant I and Poumellec B 1998 Thermal decay of gratings written in hydrogen-loaded germanosilicate fibers *Electron. Lett.* **34** 1603–4
[5] Lemaire P J and Tomita A 1984 Behavior of single mode MCVD fibers exposed to hydrogen *European Conf. on Optical Communications (Stuttgart, 1984)* pp 306–7
[6] Erdogan T, Mizrahi V, Lemaire P J and Monroe D 1994 Decay of ultraviolet-induced fiber Bragg gratings *J. Appl. Phys.* **76** 73–80
[7] Kohlrausch R 1847 Ueber das Dellmann'sche Elektrometer *Ann. Phys., Lpz.* **72** 353–405
[8] Hopkinson J 1877 The residual charge of the Leyden jar *Phil. Trans. R. Soc.* **167** 599–626
[9] Wiechert E 1893 Eine neue Methode zur Messung des Erdableitungswiederstandes von Blitzableitern *Elecktrotechnische Z.* **51** 726–7
[10] Von Schweidler E 1907 Studien uber die anomalien im verhalten der dielektrika *Ann. Phys., Lpz.*
[11] Wagner K 1913 Zur theorie der unvolkommenen dielectrica *Ann. Phys., Lpz.* **40** 817
[12] Vand V 1943 A theory of the irreversible electrical resistance changes of metallic films evaporated in vacuum *Proc. Phys. Soc.* A **55** 222–46
[13] Primak W 1955 Kinetics of processes distributed in activation energy *Phys. Rev.* B **100** 1677–89
[14] Primak W 1960 Large temperature range annealing *J. Appl. Phys.* **31** 1524
[15] Orenstein J and Kastner M 1981 Photocurrent transient spectroscopy: measurement of the density of localized states in a-AS_2Se_3 *Phys. Rev. Lett.* **46** 1421–4
[16] Tiedje T and Rose A 1980 A physical interpretation of dispersive transport in disordered semiconductors *Solid State Commun.* **37** 49–52
[17] Miller S L, McWhorter P J, Miller W M and Dressendorfer P V 1991 A practical predictive formalism to describe generalised activated physical processes *J. Appl. Phys.* **70** 4555–68
[18] Lemaire P J, Monroe D P and Watson H A 1994 Hydrogen-induced-loss increases in erbium-doped amplifier fibers: revised predictions *Optical Fiber Communication'94 (Washington, DC, USA)* ed OSA (San Jose, CA: Optical Society of America) pp 301–2
[19] Vandenbrink J P 1996 Master stress relaxation function of silica glasses *J. Non-Cryst. Solids* **196** 210–5

[20] Kannan S, Lemaire P J, Guo J and LuValle M J 1997 Reliability predictions on fiber gratings through alternate methods *Bragg Gratings Photosensitivity, and Poling in Glass Fibers and Waveguides: Applications and Fundamentals* (Williamsburg, VA: OSA) pp 52–4

[21] Poumellec B 2000 Kinetics of thermally activated processes in disordered media *POWAG 2000 (Giens, France)* ed B Poumellec, p 13 L6 (Bertrand.Poumellec@lpces.u-psud.fr)

[22] LuValle M J, Copeland L R, Kannan S, Judkins J B and Lemaire P J 1998 A strategy for extrapolation in accelerated testing *Bell Labs Tech. J.* 139–47

[23] Poumellec B 1997 Links between writing and erasure (or stability) of Bragg gratings in disordered media *Bragg Gratings Photosensitivity, and Poling in Glass Fibers and Waveguides: Applications and Fundamentals* (Williamsburg, VA: OSA) pp 178–80

[24] Abramowitz M and Stegun I A 1972 *Handbook of Mathematical Functions* (New York: Dover)

[25] Razafimahatratra D, Niay P, Douay M, Poumellec B and Riant I 2000 Comparison of isochronal and isothermal decays of Bragg gratings written through continuous-wave exposure of an unloaded germanosilicate fiber *Appl. Opt.* **39** 1924–33